Materials and Design 141 (2018) 323–332

Contents lists available at ScienceDirect

Materials and Design

journal homepage: www.elsevier.com/locate/matdes

Biphasic scaffolds of silk fibroin film affixed to silk fibroin/chitosan sponge based on surgical design for cartilage defect in osteoarthritis

Khanitta Panjapheree [a], Suttatip Kamonmattayakul [b], Jirut Meesane [a,*]

[a] Institute of Biomedical Engineering, Faculty of Medicine, Prince of Songkla University, Hat Yai, Songkhla 90110, Thailand
[b] Department of Preventive Dentistry, Faculty of Dentistry, Prince of Songkla University, Hat Yai, Songkhla 90110, Thailand

HIGHLIGHTS

- Biphasic scaffolds of silk/chitosan were created for osteoarthritis surgery.
- Biphasic scaffolds showed physical performance for osteoarthritis surgery.
- Biphasic scaffolds had biological functionality for osteoarthritis surgery.

GRAPHICAL ABSTRACT

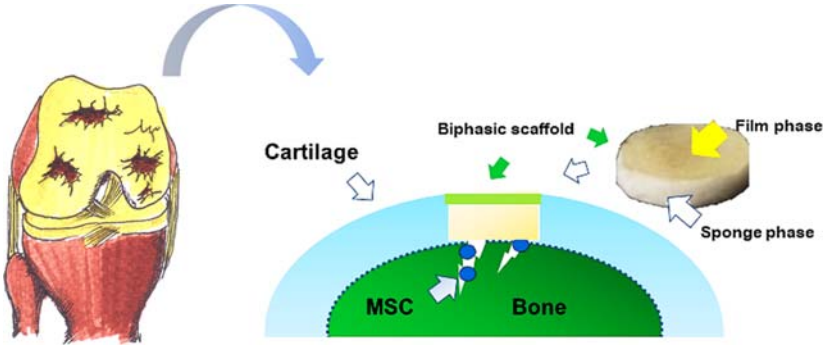

ARTICLE INFO

Article history:
Received 12 September 2017
Received in revised form 3 December 2017
Accepted 2 January 2018
Available online 03 January 2018

Keywords:
Silk fibroin
Chitosan
Biphasic scaffolds
Cartilage tissue engineering
Osteoarthritis

ABSTRACT

Osteoarthritis is inflammation that can occur at any joint, and is caused by cartilage degeneration. For severe cases, patients need surgery by substitution with performance tissue engineering scaffolds. Biphasic scaffolds of silk fibroin film affixed to a silk fibroin/chitosan sponge were constructed for osteoarthritis surgery. Silk fibroin film was fabricated before affixation to the sponge of silk fibroin/chitosan at different ratios of silk fibroin to chitosan: 100:0 (SF), 70:30 (SF70), 50:50 (SF50), 30:70 (SF30), and 0:100 (CS). The morphologies of the scaffolds were observed by scanning electron microscopy. Physical functionality as well as stability was evaluated from mechanical properties, and the percentage of swelling, and degradation. Biological functionality was evaluated using a rat mesenchymal stem cell (RMSCs) culture. Cell proliferation was analyzed and the histological structure was observed. SF30 showed suitable morphology, physical stability, and biological functionality to promote RMSC regulation into chondrocytes. This indicated that SF30 shows promise for cartilage regeneration in osteoarthritis surgery.

1. Introduction

Osteoarthritis is a degenerative disease of cartilage that results in inflammation at any joint. The loss of tissue leads to a defect that causes pain during movement. In mild cases, the patients are often treated by medications or rehabilitation [1]. In severe cases, the patients need biomaterials substitution at the defect area [2]. Therefore, the construction of biomaterials that function properly to regenerate new tissue and are suitable for surgery is a challenge for surgeons and materials scientists.

Tissue engineering scaffolds are attractive biomaterials that are used to replace defective tissue [3]. Some designs of scaffolds are able to properly regenerate new tissue in a surgical setting [4]. In the case of cartilage tissue engineering, particularly in osteoarthritis surgery,

* Corresponding author.
E-mail address: jirutmeesane999@yahoo.co.uk (J. Meesane).

https://doi.org/10.1016/j.matdes.2018.01.006
0264-1275/

Table 1
Experimental group.

Groups	Detail
SF	Silk fibroin film affixed to silk fibroin/chitosan sponge (100:0)
SF70	Silk fibroin film affixed to silk fibroin/chitosan sponge (70:30)
SF50	Silk fibroin film affixed to silk fibroin/chitosan sponge (50:50)
SF30	Silk fibroin film affixed to silk fibroin/chitosan sponge (30:70)
CS	Silk fibroin film affixed to silk fibroin/chitosan sponge (0:100)

some scaffolds were designed into biphasic scaffolds of bone/cartilage [5]. These scaffolds have two phases. The first phase is put in bone and the second phase contacts with cartilage. To apply these designed scaffolds in surgery practice, the surgeons prepare the area for substitution by removal of cartilage tissue at the defect site and cut a suitable hole in the bone. The biphasic scaffold of bone/cartilage is then put into the prepared area [6]. To put the scaffold in the prepared area, the bone phase of the biphasic scaffold is plugged into the hole. The bone phase of the biphasic scaffold acts as the fixation [7]. The cartilage phase of biphasic scaffolds functions to maintain the shape at the cartilage defect area [8]. In this technique, the bone and cartilage cells are co-cultured in the biphasic scaffolds before transplant into the defect area [9]. However, this technique is a complicated surgical procedure.

An interesting design of scaffolds used for osteoarthritis surgery is the use of membranes [10]. After removal of the defect in cartilage tissue, the bone is punched into a microfracture that acts as a channel for the migration of mesenchymal stem cells (MSCs) [11]. The area where the cartilage defect was removed is then covered by the membrane which acts as guidance for cartilage tissue regeneration [12]. In this case, stem cells migrate into the area that was removed and self-regulate into chondrocytes [13]. The membrane also serves as a barrier to prevent migration of stem cells from the microfracture to the outside of the defect site [14]. The side in contact with the stem cells has a high degree of roughness and biological function that is suitable for cartilage tissue regeneration [15]. The popular membrane for osteoarthritis surgery is collagen which exhibits a high degradation rate that is a disadvantage of the membrane [16]. Rapid degradation causes migration of stem cells to the outside and reduces signals to the inside of the defect area. Therefore, the design and construction of suitable membrane scaffolds for cartilage tissue engineering for osteoarthritis surgery is the focus of this research.

Silk fibroin is a natural polymer used often in biomedical applications [17]. Silk fibroin has been used for the construction of scaffolds in tissue engineering due to its superior mechanical and physical properties [18]. For cartilage tissue engineering, some research fabricated silk fibroin into three dimensional (3D) scaffolds for transplantation into a defect tissue site of cartilage particularly in osteoarthritis disease [19,20,21,22]. The silk fibroin scaffolds were able to maintain the shape at the defect site and induce tissue regeneration [23]. Because of the high performance, silk fibroin was selected as the base material for the design and construction of scaffolds for cartilage tissue engineering in osteoarthritis surgery in this research.

Chitosan is a modified natural polymer that functions biologically to induce tissue regeneration [24]. Therefore, chitosan is used often in the fabrication of scaffolds for tissue engineering [25]. For cartilage tissue engineering, chitosan was constructed into 3D scaffolds that had suitable biological performance to induce tissue regeneration [26]. Due to those characteristics, chitosan was selected in combination with silk fibroin for the design and construction of scaffolds for cartilage tissue engineering [27,28].

In this research, silk fibroin and chitosan were chosen as the materials for the design and construction of biphasic membrane scaffolds. The morphology, physical stability, and biological functionality of the scaffolds were evaluated for promise in cartilage defect, particularly in osteoarthritis surgery.

2. Materials and methods

2.1. Preparation of silk fibroin aqueous solution

Silk fibroin (SF) was provided by Queen Sirikit Sericulture Center, Narathiwat, Thailand. The SF fiber (*Bombyx mori*) was boiled in a 0.02 M sodium carbonate (Na_2CO_3) solution for 20 min. The sericin was then removed by washing with distilled water. The dried silk fibroin fiber was dissolved in a 9.3 M lithium bromide solution (LiBr) at 70 °C for 150 min. Finally, a purified SF solution was obtained using distilled water which was changed every 6 h for 3 days and centrifuged at 9000 RPM for 20 min.

2.2. Preparation of chitosan aqueous solution

Chitosan (CS) powder (MW 1700 kDa, degree of deacetylation >90%, Marine Bio Resources Co., Ltd) was dissolved in 0.1 M acetic acid. CS solutions were stirred until completely dissolved and filtered to remove any insoluble chitosan powder.

2.3. Preparation of the silk fibroin film

A quantity of 4 mL of SF was poured into a plastic box (3 × 3 cm) and allowed to stand for 2 days at room temperature to allow the film to dry

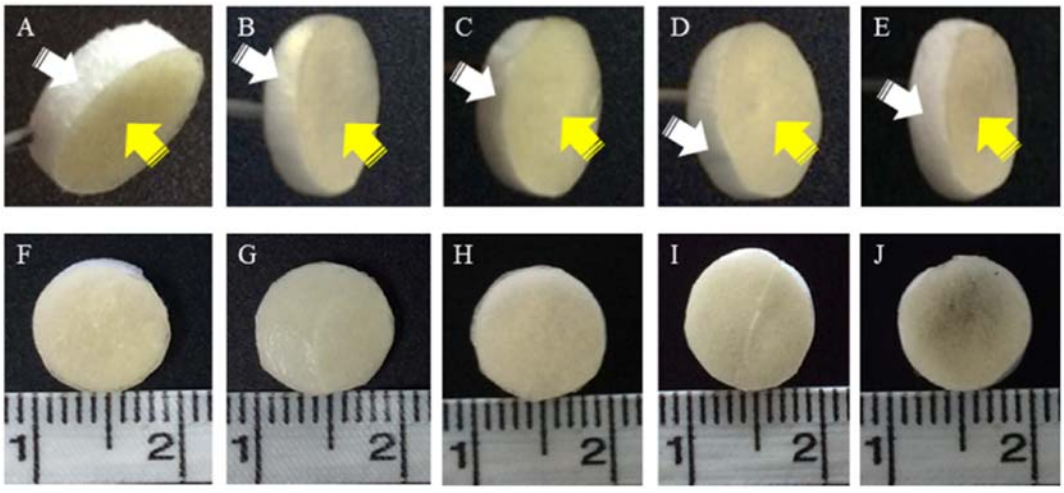

Fig. 1. Constructed biphasic scaffolds: A,F) SF; B,G) SF70; C,H) SF50; D,I) SF30; and E,F) CS. Yellow arrows indicate silk fibroin films. White arrows indicate silk fibroin/chitosan sponges. (For interpretation of the references to colour in this figure legend, the reader is referred to the web version of this article.)

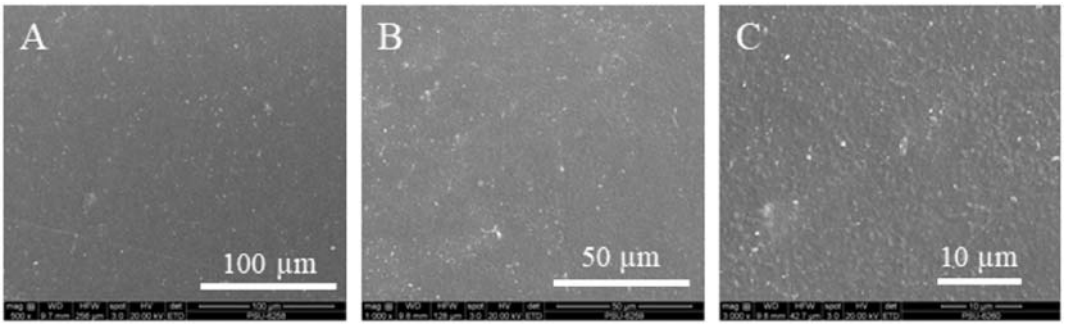

Fig. 2. Morphology of silk fibroin film under different magnification: A) ×500, B) ×1000, and C) ×2000.

before immersing in methanol to transform random coil to beta sheet structure. The film was cut into 1 × 1 cm pieces for testing.

2.4. Preparation of the porous phase of silk fibroin/chitosan

A 3% SF solution was combined with a 3% CS solution in the ratios of 100:0, 70:30, 50:50, 30:70, and 0:100. About 1 mL of each solution was added into 48 well plates. Finally, the plates were lyophilized for freeze-drying, allowed to dry, and immerse in methanol to transform random coil to beta sheet structure. Then, samples were cut into 2 × 10 mm disks.

2.5. Construction of biphasic scaffolds

The dried SF film was cut into diameter of 10 mm disk. Then, the silk fibroin film was affixed to the porous phase of the silk fibroin/chitosan scaffold by gluing with a silk solution and allowed to sit at room temperature for 2 days to complete the firm construction of the biphasic scaffolds (see Table 1).

2.6. Scanning electron microscope (SEM)

The morphologies of the scaffolds were observed by a scanning electron microscope (Quanta400, FEI, Czech Republic). The samples were coated with gold dust on the surface and observed at a magnification of 3000×.

2.7. Pore size diameter and distribution of scaffold

The image of morphology from SEM was used to analyze pore size analysis. ImageJ was applied to use for pore size measurement with randomly area selection ($n = 25$) [29]. Then, the obtained data was calculated and plotted by Qtiplot program.

2.8. Mechanical properties

The compressive strength of all scaffolds, in dry conditions, was tested with a universal testing machine (Lloyd model LRX-Plus, Lloyd Instrument Ltd., London, UK). All scaffolds were cut into a diameter of; 10 mm, at a thickness of 5 mm. For testing conditions, the scaffolds were compressed with a static load cell of; 250 N, at a rate of 2 mm/min, which was stopped at a strain of 40%.

2.9. Percentage of swelling

Each group was weighed and immersed in a phosphate-buffered saline (PBS) solution at room temperature for 1, 3, 5, and 7 days. The swelling ratios were calculated from the following equation:

$$\% \text{ Swelling} = \frac{(W_s - W_d) \times 100}{W_d}$$

W_s = Weight of a swollen scaffold
W_d = Weight of a dry scaffold

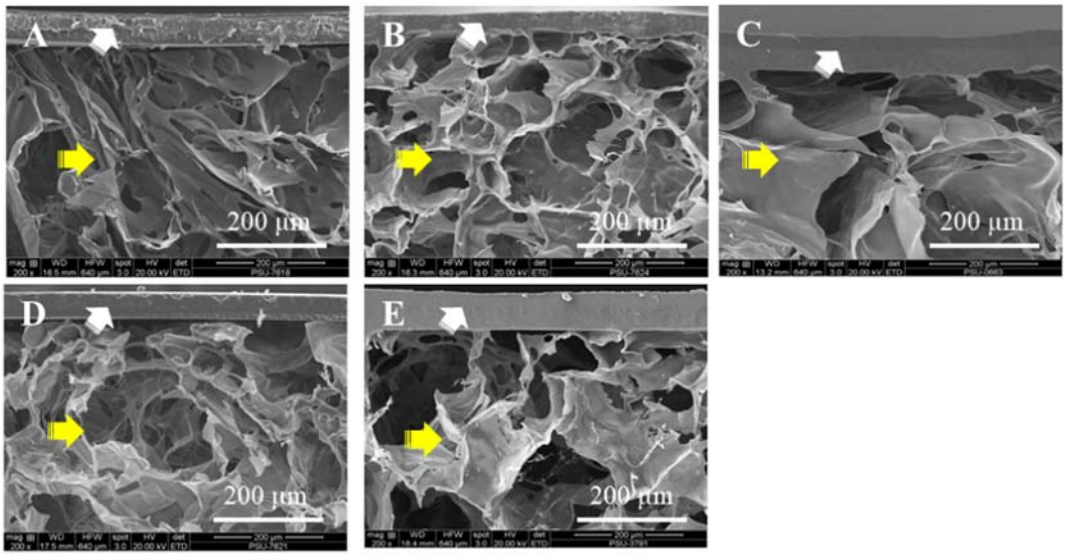

Fig. 3. Morphology of the constructed biphasic scaffolds: A) SF; B) SF70; C) SF50; D) SF30; and E) CS. White and yellow arrows indicated films and porous phase, respectively. (For interpretation of the references to colour in this figure legend, the reader is referred to the web version of this article.)

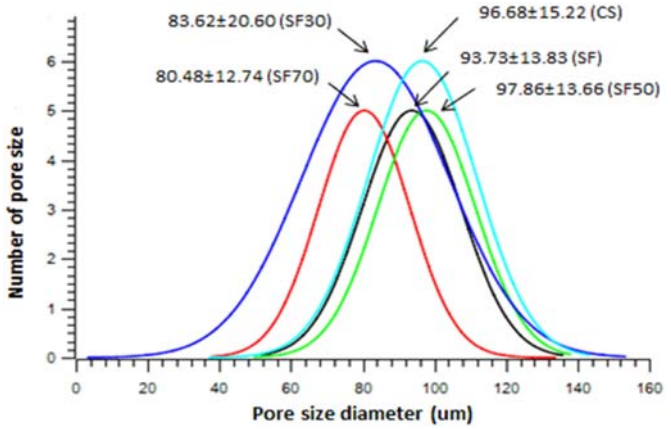

Fig. 4. Pore size and distribution of the constructed biphasic scaffolds: A) SF; B) SF70; C) SF50; D) SF30; and E) CS.

2.10. Biodegradation

The scaffolds of all groups were immersed in a 4 mg/mL lysozyme solution (pH 7.4) and incubated at 37 °C for 1, 2, 3, and 4 weeks. The appearance of all scaffolds was observed each week. The scaffolds were washed with distilled water for freeze-drying and the % weight loss was calculated by this equation:

$$\%\text{Weight loss} = \frac{(\text{Initial weight–Weight after degradation}) \times 100}{\text{Initial weight}}$$

2.11. Cell culture

Rat mesenchymal stem cells (RMSC) were cultured in a 75 cm^3 flask with rat mesenchymal stem cell growth medium (Cell Applications, Inc., US & Canada). The RMSC were kept in a 37 °C incubator with 5% CO_2 and the media was changed every 2 days. The RMSC were seeded in all biphasic scaffolds with 2×10^6 cells and cultured for 7 days. Then, the RMSC were induced with the StemPro® Chondrogenesis Differentiation Kit (Gibco, Invitrogen, Carlsbad, CA, USA) for chondrocyte differentiation of the RMSC.

2.12. Stem cell proliferation (PrestoBlue at days 1, 3, 5, and 7)

Stem cell proliferation on the biphasic scaffolds was measured on days 1, 3, 5, and 7 using PrestoBlue (PrestoBlue® Cell Viability Reagent, Invitrogen, USA) reagent. The biphasic scaffolds were washed 2 times with PBS solution. The prepared PrestoBlue solution by mixing with the fresh media at the ratio of 1:10 and then added into the biphasic scaffolds. The biphasic scaffolds were incubated for 1 h at 37 °C and measured at a wavelength of 600 nm emission.

2.13. Histology analysis (days 7 and 14)

After inducing the RMSC, the cell cultured biphasic scaffolds were fixed overnight in 4% formaldehyde in buffered PBS (pH 7.4), embedded in paraffin, and cut into 5 μm sections. The sections were deparaffinized and stained with hematoxylin and eosin (H&E) to determine the cellular morphologies. Alcian, blue staining was used to evaluate the synthesis of glycosaminoglycans (GAGs). This; blue dye, in alcian blue staining, detects any cartilaginous tissue. In addition to this, Masson's trichrome staining was used to observe the synthesis of collagen type II.

2.14. Statistical analysis

Five samples ($n = 5$) were used for testing. All data were measured and statistically compared by one-way ANOVA followed by Tukey's HDS test (SPSS 16.0 software package). The results were reported as mean ± standard deviation. Statistical significance was defined as $^*p < 0.05$.

3. Results

3.1. Morphological structure of constructed biphasic scaffolds

The appearances and morphological structures of the constructed biphasic scaffolds were observed (Figs. 1, 2, and 3.). There were no differences in the appearance of the scaffolds. The scaffolds were composed of two phases: silk fibroin fim and silk fibroin/chitosan sponge which was prepared in different ratios. The silk fibroin films were smooth and transparent. The sponge phase of the scaffolds had a rough surface and were turbid. The evaluation of the morphological structure demonstrated that the silk fibroin films were affixed to the sponge part of the silk fibroin/chitosan. During the film phase, the morphology displayed a dense surface, as well as which, during this, phase it had both a smooth surface and rough surface, at both low and high magnification, respectively. In the spongy phase, the morphology was a porous structure which had a rough wall. Furthermore, some areas of those pores had small fibril internal networks. The morphological formation of the films and spongy phase were not different.

Results of the morphological studies indicated no differences in any of the scaffolds at the zone of attachment. The silk fibroin films and porous phases had good adhesion. The silk fibroin solution possibly diffused into the textures of the silk fibroin film and porous phase [30] which decreased the surface tension between the film and porous

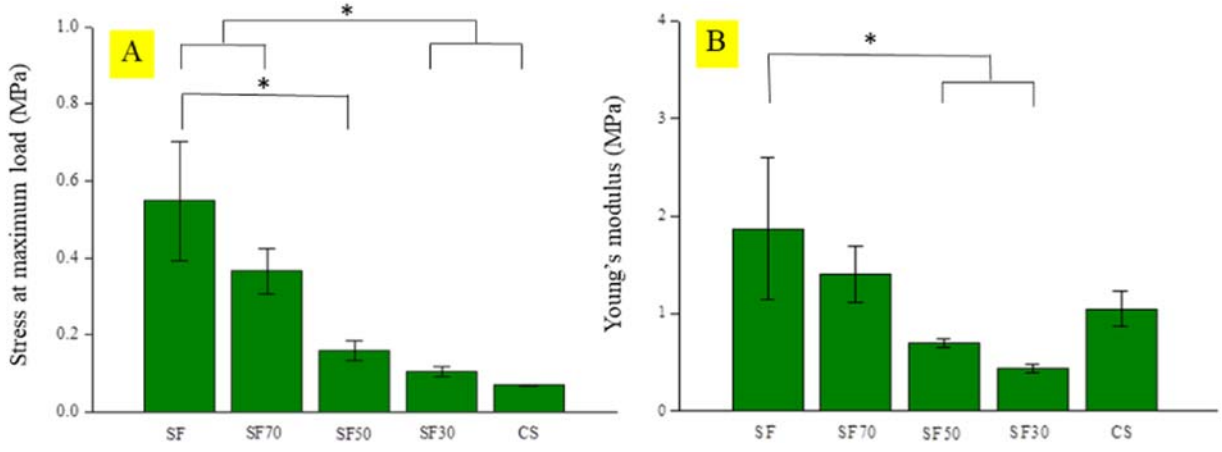

Fig. 5. Mechanical properties of the constructed biphasic scaffolds: A) Stress at maximum load B) Young's modulus.

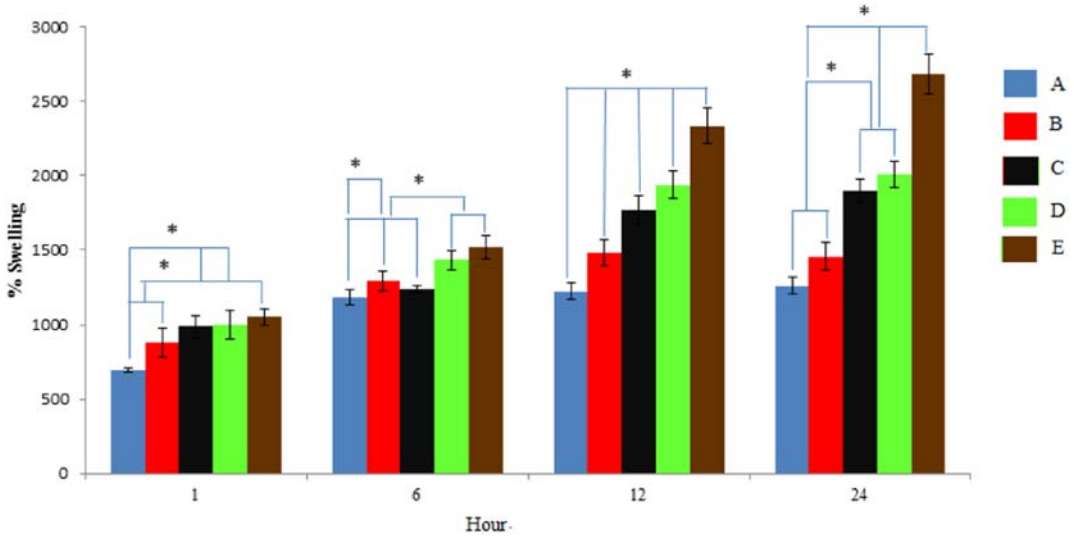

Fig. 6. Swelling percentage of the constructed biphasic scaffolds; A) SF; B) SF70; C) SF50; D) SF30; and E) CS at 1, 6, 12, and 24 h.

phases [31]. This led to fusion at the connection zone via physical interaction [32].

3.2. Pore size and distribution of constructed biphasic scaffolds

To clarify the further details of morphology, the pore size and distribution were measured and analyzed. Pore size of; SF, SF70, SF50, SF30, and CS showed; 93 ± 13.83, 80.48 ± 12.74, 97 ± 13.66, 83.62 ± 20.60, 96.68 ± 15.22 μm, respectively (Fig. 4). The pore size shows that for SF50 > CS > SF > SF30 > SF70. The results demonstrated that SF50 had the largest pore size, with all pore size distributions being: SF, SF70, SF50, SF30, and CS was 46–128, 40–128, 46–140, 0–146, and 40–146 μm. The distribution range of pore sizes demonstrated that; SF30 > CS > SF50 > SF70 > SF. These results also indicated that; SF30 had the longest range of pore size distribution.

3.3. Mechanical properties of constructed biphasic scaffolds

Mechanical properties of constructed, biphasic scaffolds were presented with stress at a maximum load, with Young's modulus (Fig. 5). The stress, at maximum load, shows that for SF > SF70 > SF50 > SF30 > CS. SF and SF70 had more stress at maximum load than that of SF50, SF30, and CS. The results additionally demonstrated that; the stress at maximum load decreased as the percentage of chitosan increased. Young's modulus of SF50 and SF30 were lower than the others. Young's modulus of silk fibroin/chitosan decreased when the amount of chitosan increased.

Fig. 7. Degradation of constructed biphasic scaffolds at days 7, 14, and 21.

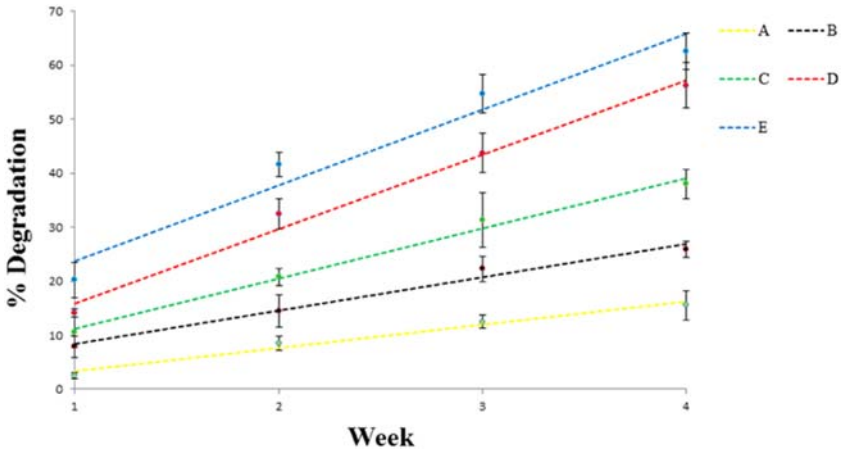

Fig. 8. Degradation percentage of constructed biphasic scaffolds: A) SF; B) SF70; C) SF50; D) SF30; and E) CS.

3.4. Swelling behavior of constructed biphasic scaffolds

Swelling behavior was selected to evaluate the physical stability. The results showed that SF70, 50, 30, and CS had higher percentage of swelling than the SF at 1 h (Fig. 6). At 6 h, the SF30 and CS scaffolds showed higher percentage of swelling than the SF50, 70, and SF. After 12 to 24 h, steady state was attained and the percentage of swelling of the biphasic scaffolds increased as the percentage of chitosan increased. The SF showed the lowest percentage swelling while CS had the highest percentage of swelling.

3.5. Degradation of constructed biphasic scaffolds

Physical stability of biphasic scaffolds was evaluated by testing the degradation with lysozyme. At day 7 of testing, the results showed that SF, SF70, SF50, and SF30 could hold the contour shape (Fig. 7). The SF30 showed some areas of degradation in the texture. CS showed much deformation and degradation in the texture. At day 14, SF, SF70, SF50, and SF30 could hold the contour shape. SF30 showed increased degradation in the texture. CS showed deformation of the contour shape and much degradation of the texture. At day 21, SF, SF70, and SF50 could hold the contour shape. There were some areas which were degraded in the texture of SF70 and SF50. The SF30 and CS appeared to have a deformed contour shape and much texture degradation.

The quantification of degradation percentage is shown in Fig. 8. The results demonstrated that CS had the highest amount of degradation. SF showed the lowest amount of degradation. The degradation increased as the amount of chitosan increased. The SF30 and CS scaffolds showed higher degradation rates than the others.

3.6. Stem cell proliferation on constructed biphasic scaffolds

Stem cell proliferation was analyzed at days 1, 3, 5, and 7 to evaluate the biological performance (Fig. 9). The results demonstrated that all

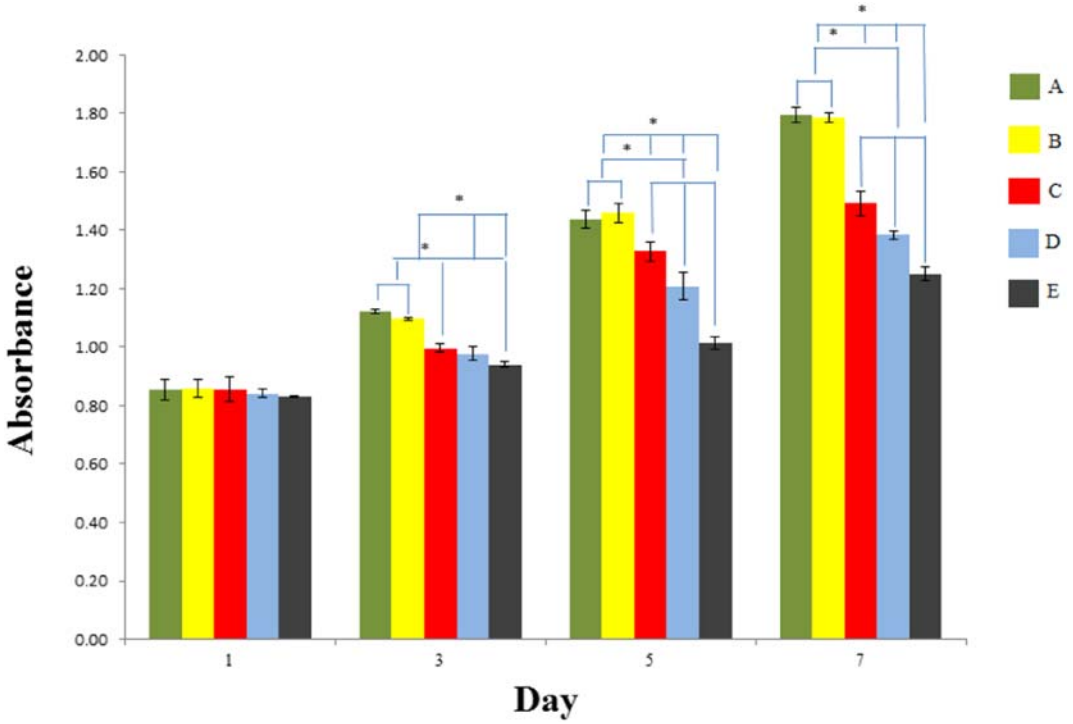

Fig. 9. Cell proliferation of on the constructed biphasic scaffolds: A) SF; B) SF70; C) SF50; D) SF30; and E) CS at days 1, 3, 5, and 7.

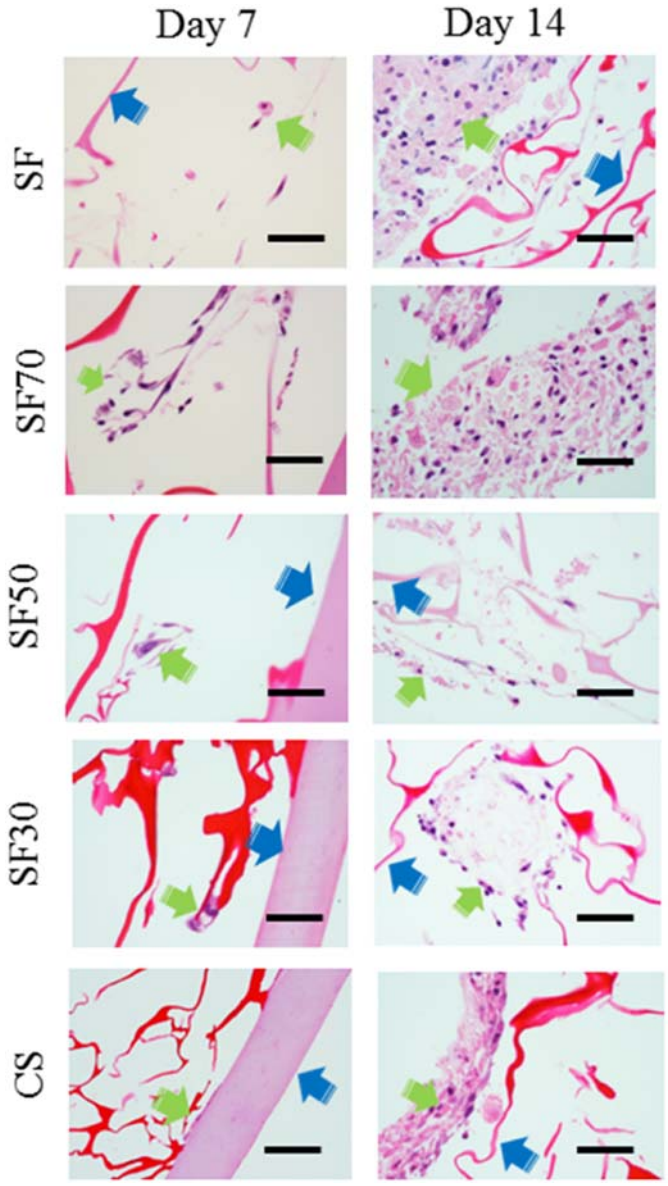

Fig. 10. Histological structure of cultured biphasic scaffolds with H&E staining at days 7 and 14. Green and blue arrows indicate cells and scaffolds, respectively. Scale bar = 100 μm. (For interpretation of the references to colour in this figure legend, the reader is referred to the web version of this article.)

samples had increased proliferation over time. The results showed no differences of cell proliferation in all samples at day 1. At days 3, 5, and 7, the SF and SF70 scaffolds had higher proliferation than the others and CS had the lowest amount of cell proliferation. There were no differences between SF50 and SF30 at day 3. The SF50 scaffold showed higher cell proliferation than SF30 at day 5 and 7.

3.7. Histological structure of cell cultured biphasic scaffolds

In this research, morphological formation of cultured biphasic scaffolds was observed by histology at days 7 and 14 (Fig. 10). At day 7, the results showed that SF and SF70 demonstrated more cell adhesion on the porous scaffolds than the others. The SF70 showed aggregation of cell adhesion in the pores of the scaffold. The SF50 and CS scaffolds had a little cell adhesion in the pores. At day 14, the results demonstrated that SF and SF70 displayed self-organized cells in a dense structure. The dense structure attached to the pores. The SF50 scaffold had thin layers of cell adhesion in the pores. SF30 displayed self-organized cells in spheroid formation in the pores. CS showed cell layers which attached in the pores.

The biological performance of the scaffolds was evaluated from the stained GAGs which were secreted from the cells. The GAGs are biomarkers of cartilage tissue formation. The results showed glycosaminoglycans which adhered on the scaffolds (Fig. 11). At day 7, SF70 showed secreted glycosaminoglycans more clearly than the others. The CS showed the least amount of secreted glycosaminoglycans on the scaffold. At day 14, the secreted glycosaminoglycans of SF and SF70 were embedded in the dense structure. The SF50, 30, and CS scaffolds showed the formation of loose networks of secreted glycosaminoglycans in the pores.

Collagen type II is an important marker, which represents cartilage tissue formation. The results showed that; SF, SF70, SF50, SF30, and CS had cells as well as collagen type II adhered on the surface of the pores at both; day 7 and day 14 (Fig. 12). At day 7, there were some small clusters of collagen type II distribute in the porous structures of the scaffolds. There were no differences of collagen type II organization for all samples, at this time point, however, at day 14 the collagen type II

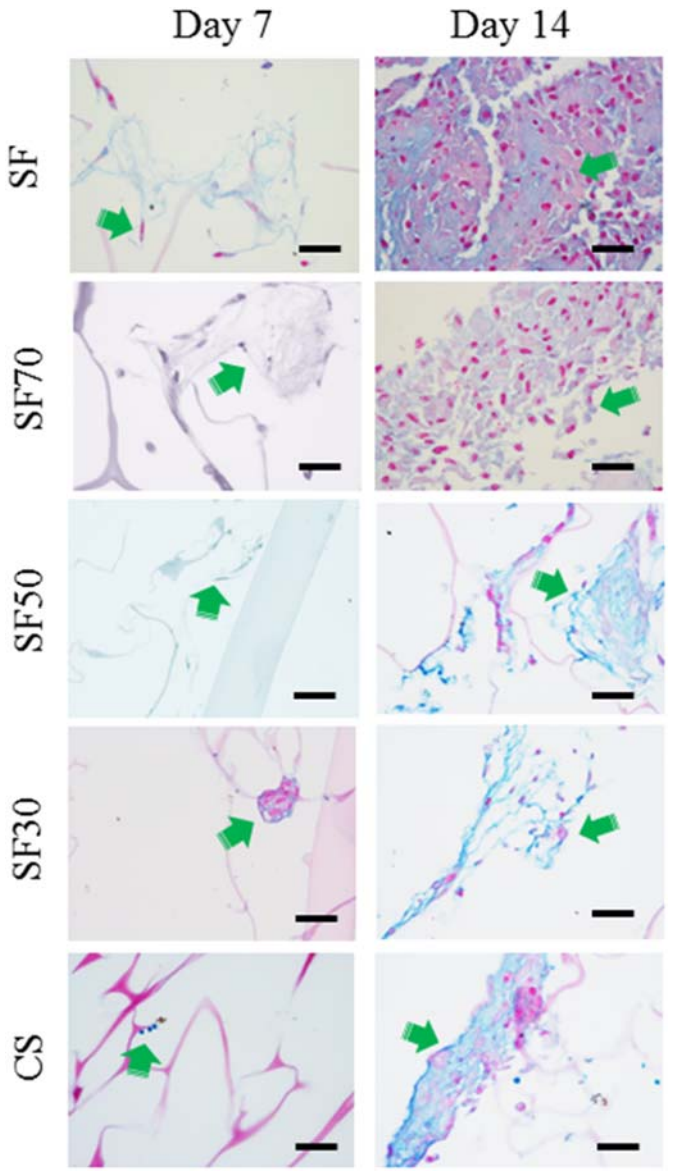

Fig. 11. Histological structure of cultured biphasic scaffolds with alcian blue staining at days 7 and 14. Green arrows indicate secreted GAGs from the cells. Scale bar = 100 μm. (For interpretation of the references to colour in this figure legend, the reader is referred to the web version of this article.)

organized themselves into large aggregation in the porous structures. The results indicated that; SF70, SF50, SF30 and CS showed larger aggregation than that of SF.

4. Discussion

4.1. Morphological formation of constructed biphasic scaffolds

In this research, biphasic scaffolds were proposed for guidance cartilage tissue regeneration. In the surgical approach, the debris of a cartilage defect is removed to the subchondral bone before making microcracks which are the channels for migration of bone marrow stem cells (MSCs) into the debrided area of cartilage. Generally, the debrided area has a microenvironment which can regulate MSCs into chondrocytes. To induce the performance for MSCs regulation at the debrided area, the spongy phase of those scaffolds was proposed to be in contact with the MSCs. Suitable porous structures and characteristics act as the physical and biological clues to guide and enhance cartilage tissue regeneration. On the other hand, the silk fibroin film generally provided physical stability and performed as a barrier. Therefore, silk fibroin film was proposed to protect the leakage of MSCs into the synovial fluid. Furthermore, the silk fibroin film has a suitable barrier function to prevent migration of some cells and signals which disturb tissue regeneration. Therefore, for surgery, the silk fibroin film was proposed to be in contact with the synovial fluid.

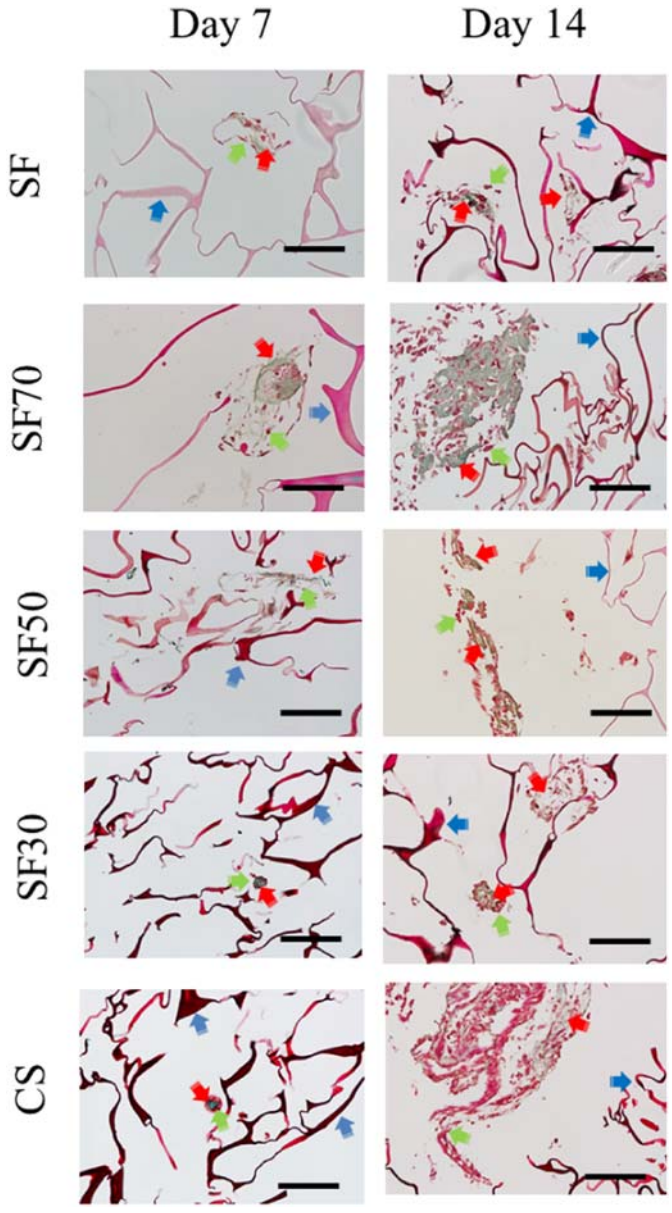

Fig. 12. The histological structures of cultured, biphasic scaffolds, with the use of Masson's trichrome staining at days 7 and 14. The red, green, and blue arrows indicate collagen type II, the cells, and the scaffolds, respectively. Scale bar = 100 μm. (For interpretation of the references to colour in this figure legend, the reader is referred to the web version of this article.)

In this research, the morphology of the spongy phase is the main part to be in contact with the MSCs. The spongy phase of those scaffolds exhibited a porous formation which was generated from freeze-drying. The porous structure had an internal fibril network. This was possibly form different ice crystal formations in the silk fibroin and chitosan. In some cases, the ice crystal formation acts as a template and is the cause of the fibril network formation or a sophisticated structure in the porous structure after freeze-drying. Interestingly, some research demonstrated that the network structure and sophisticated structure in the pores can promote cell adhesion, proliferation, and migration which lead to the induction of tissue regeneration. Therefore, the network structure in the pores of the spongy phase for those scaffolds possibly has the performance to promote cell adhesion, proliferation, and migration.

From morphological observations, the results revealed similar morphologies, which may have possibly had no effect on the functionality of these scaffolds. Moreover, when analyzed the pore size as well as distribution, showed that there were non-distinguish differences of SF and CS. Notably, the pore size, and distribution did show differences, and irregular trends of silk fibroin/chitosan. The characteristics and ratios of the silk fibroin/chitosan scaffolds might be the main effect on the functionality of the scaffolds. However, there is no proof of this hypothesis. Evaluations of the physical stability and biological functionality of the scaffolds were undertaken.

4.2. Physical functionality, and stability of constructed, biphasic scaffolds

In this research, mechanical properties, the swelling behavior, and degradation with lysozyme evaluated the physical functionality as well as stability of the constructed, biphasic scaffolds.

Firstly, the mechanical properties were used to evaluate physical functionality for the design of these biphasic scaffolds. The results demonstrated that; silk fibroin, without chitosan, had higher stress at a maximum load, and Young's modulus than silk fibroin with chitosan. Additionally, the silk fibroin/chitosan scaffolds showed a decrease of stress and modulus with increasing amounts of chitosan. This inferred that; silk fibroin/chitosan expresses soft characteristic, which act as the physical clues in inducing MSCs regulation into chondrocyte, much the same as in native, cartilage tissue.

Secondly, the swelling behavior was selected to evaluate the guidance for design of the performance of the scaffolds to be similar to the hydrogel characteristics of cartilage tissue [33]. Based on the results, the constructed biphasic scaffolds which had a high amount of chitosan had greater swelling than the scaffolds with a low amount of chitosan. This comes from the hydrophilicity of chitosan which can maintain a high amount of water [34]. The results also indicated that the constructed biphasic scaffolds with a high amount of chitosan had lower physical stability. Generally, cartilage tissue can maintain a high water content that results from the hydrophilic hyaluronic acid (HA) in its structure [35]. Some research demonstrated that the HA affected the spheroid formation of stem cells [36]. Therefore, optimizing chitosan content might be a clue to regulate the stem cells into spheroid formation of chondrocytes in cartilage tissue.

In addition to this, the results showed higher degradation of scaffolds with chitosan than without chitosan. This indicated that scaffolds with a high content of chitosan had low physical stability. Some reports demonstrated that scaffolds with different physical stabilities due to degradation are suitable for different types of tissue regeneration [37].

Therefore, optimized degradation of a scaffold that is suitable for tissue regeneration is important in the design of scaffolds. Some research reported that a given rate of scaffold degradation should act as a physical clue for cell regulation into spheroid organization [38].

Based on the mechanical properties, swelling, degradation of the scaffolds, with a specific amount of chitosan, possibly shows physical clues, which can regulate stem cells into spheroid organization. This is suitable as a guide for cartilage tissue regeneration for osteoarthritis surgery. However, to prove this hypothesis, biological functionality was undertaken.

4.3. Biological functionality of constructed biphasic scaffolds

In this research, cell proliferation, and the histological structure of the cultured scaffolds were presented to evaluate biological functionality. First, the scaffolds without chitosan and with a low amount of chitosan exhibited higher cell proliferation than higher amounts of chitosan. This possibly came from the physical stability of those scaffolds. The scaffolds without chitosan and with a low amount of chitosan had greater stability than the higher amounts chitosan. Some research showed that the physical stability of scaffolds has an effect on the induction of cell adhesion [39]. Furthermore, some amino acids in silk fibroin demonstrated the functionality of cell recognition [40]. This led to enhanced cell proliferation [41].

Second, the histology of cultured scaffolds was observed to evaluate the biological functionality. There was self-organization of cells on scaffolds with different amounts of chitosan. The scaffolds without and with a low amount of chitosan demonstrated unique cell adhesion in the early stages of culturing and self-organized into a dense structure in the later stages. Thus, the physical stability of the scaffolds had an effect on the enhancement of cell adhesion and dense structural formation. On the other hand, the scaffolds with a high amount of chitosan had poor cell adhesion on the scaffolds in the early stages. In the later stages, the cells self-organized into a loose network formation in the SF50 scaffold and layer formation in the CS scaffold. The cells self-organized into a spheroid formation in the SF30 scaffold. This possibly resulted from the low amount of silk fibroin which acted as the structural part as collagen fibril for cell adhesion in the early stages [42]. On the other hand, a high amount of chitosan acts as the elastic texture part of HA which can promote cell mobility [43,47]. The elastic texture can promote spheroid formation similar to chondrocytes in cartilage tissue [44].

Secreted GAGs serve as a biomarker of regulation of MSCs into chondrocytes. The results showed secreted GAGs that adhered to the porous structure for all scaffolds. However, the results of secreted GAGs varied. For the SF and SF70 scaffolds, more GAGs were secreted than the scaffolds with higher amounts of chitosan in the early stages of cell culture. This possibly indicated that the physical stabilities and of SF and SF70 acted as firm substrates for deposition of the secreted GAGs. Furthermore, SF and SF70 might have the role to activate the secretion of GAGs. In the later stages, the secreted GAGs of SF and SF70 embedded in the dense structure of cell organization. This showed an irregular organization in cartilage tissue [45,48]. On the other hand, the SF50, SF30, and CS scaffolds exhibited loose secreted GAGs in the porous structures. This was similar to native regular GAGs formation in cartilage tissue [46].

Collagen type II is an important marker that; refers to cartilage tissue formation. Generally, collagen type II is secreted from MSCs that then regulate themselves into chondrocytes. Interestingly, the physical clues have an important role in the enhancement of this regulation. According to the results, the scaffolds of silk fibroin, with chitosan, demonstrated physical clues that could activate the enhancement of collagen type II secretion similar to that of native, cartilage tissue formations. Notably, SF30 showed that; MSCs self-organized into a spheroid formation, which is similar to the organization of chondrocyte within native, cartilage tissue.

The results of the biological, functionality evaluation indicated that the scaffolds with a specific ratio of silk fibroin/chitosan sponge, particularly in SF30, had suitable cell proliferation, a spheroid formation, a loose, secreted GAG formation, and collagen type II organization. This showed suitable biological functionality which can lead to tissue formation similar to native cartilage.

5. Conclusion

In this research, biphasic scaffolds of silk fibroin film affixed to a silk fibroin/chitosan sponge were designed and constructed to use as a guide for cartilage tissue regeneration in osteoarthritis surgery. The results demonstrated that the designed and constructed biphasic scaffolds which had high amounts of chitosan, particularly in the SF30 scaffold, had the morphology, physical functionality, stability, and biological functionality which could maintain the contour shape and promote spheroid formation of MSCs. This indicated that SF30 shows promise in cartilage tissue regeneration for osteoarthritis surgery.

Acknowledgments

This work was partially supported by project EC 60-208-25-2 from the Graduate School and Institute of Biomedical Engineering, Faculty of Medicine, Prince of Songkla University. Many thanks go to Queen Sirikit Sericulture Centre, Narathiwat, Thailand for the supply of silk fibroin in this research.

References

[1] C. Cavallo, G. Desando, A. Facchini, B. Grigolo, Chondrocytes from patients with osteoarthritis express typical extracellular matrix molecules once grown onto a three-dimensional hyaluronan-based scaffold, J. Biomed. Mater. Res. A 93 (1) (2010) 86–95.
[2] H. Ohgushi, N. Noriko Kotobuki, H. Funaoka, H. Machida, M. Hirose, Y. Tanaka, Y. Takakura, Tissue engineered ceramic artificial joint—ex vivo osteogenic differentiation of patient mesenchymal cells on total ankle joints for treatment of osteoarthritis, Biomaterials 26 (22) (2005) 4654–4661.
[3] F.J. O'Brien, Biomaterials & scaffolds for tissue engineering, Mater. Today 14 (3) (2011) 88–95.
[4] U.A. Stock, J.P. Vacanti, Tissue engineering: current state and prospects, Annu. Rev. Med. 52 (1) (2001) 443–451.
[5] J.J. Li, D.L. Kaplan, H. Zreiqat, Scaffold-based regeneration of skeletal tissues to meet clinical challenges, J. Mater. Chem. B 2 (14) (2014) 7272–7306.
[6] J.J. Li, K. Kim, S.I. Roohani-Esfahani, J. Guo, D.L. Kaplan, H. Zreiqat, A biphasic scaffold based on silk and bioactive ceramic with stratified properties for osteochondral tissue regeneration, J. Mater. Chem. B 3 (26) (2015) 5361–5376.
[7] S. Panseri, A. Russo, C. Cunha, A. Bondi, A. Di Martino, S. Patella, E. Kon, Osteochondral tissue engineering approaches for articular cartilage and subchondral bone regeneration. Knee surgery, sports traumatology, Arthroscopy 20 (2012) 1182–1191.
[8] S.J. Seo, C. Mahapatra, R.K. Singh, J.C. Knowles, H.W. Kim, Strategies for osteochondral repair: focus on scaffolds, J. Tissue Eng. Regen. Med. 5 (1) (2014) 1–14.
[9] C.H. Chang, F.H. Lin, C.C. Lin, C.H. Chou, H.C. Liu, Cartilage tissue engineering on the surface of a novel gelatin–calcium-phosphate biphasic scaffold in a double-chamber bioreactor, J. Biomed. Mater. Res., Part B 71B (2004) 313–321.
[10] M. Keeney, A. Pandit, The osteochondral junction and its repair via bi-phasic tissue engineering scaffolds, Tissue Eng. B Rev. 15 (1) (2009) 55–73.
[11] J.P. Benthien, P. Behrens, The treatment of chondral and osteochondral defects of the knee with autologous matrix-induced chondrogenesis (AMIC): method description and recent developments, Knee Surg. Sports Traumatol. Arthrosc. 19 (8) (2011) 1316–1319.
[12] J.P. Benthien, P. Behrens, Autologous matrix-induced chondrogenesis (AMIC): combining microfracturing and a collagen I/III matrix for articular cartilage resurfacing, Cartilage 1 (1) (2010) 65–68.
[13] D.A. Grande, S.S. Southerland, R. Manji, D.W. Pate, R.E. Schwartz, P.A. Lucas, Repair of articular cartilage defects using mesenchymal stem cells, Tissue Eng. 1 (4) (1995) 345–353.
[14] S.G. Kim, M.K. Kim, H.Y. Kweon, Y.Y. Jo, K.G. Lee, J.K. Lee, Comparison of unprocessed silk cocoon and silk cocoon middle layer membranes for guided bone regeneration, Maxillofac. Plast. Reconstruct. Surg. 38 (1) (2016) 1–11.
[15] B.D. Boyan, J. Lincks, C.H. Lohmann, V.L. Sylvia, D.L. Cochran, C.R. Blanchard, D.D. Dean, Z. Schwartz, Effect of surface roughness and composition on costochondral chondrocytes is dependent on cell maturation state, J. Orthop. Res. 17 (1999) 446–457.

[16] P. Cherubino, F.A. Grassi, P. Bulgheroni, M. Ronga, Autologous chondrocyte implantation using a bilayer collagen membrane: a preliminary report, J. Orthop. Surg. 11 (1) (2003) 10–15.
[17] M. Floren, C. Migliaresi, A. Motta, Processing techniques and applications of silk hydrogels in bioengineering, J. Function. Biomater. 7 (3) (2016) 1–22.
[18] A.M. Ghaznavi, L.E. Kokai, M.L. Lovett, D.L. Kaplan, K.G. Marra, Silk fibroin conduits: a cellular and functional assessment of peripheral nerve repair, Aesthet. Plast. Surg. 66 (3) (2011) 273–279.
[19] C. Foss, E. Merzari, C. Migliaresi, A. Motta, Silk fibroin/hyaluronic acid 3D matrices for cartilage tissue engineering, Biomacromolecules 14 (14(1)) (2013) 38–47.
[20] A. Shamsa, A. Zamanian, M. Mozafari, Super-paramagnetic responsive silk fibroin/chitosan/magnetite scaffolds with tunable pore structures for bone tissue engineering applications, Mater. Sci. Eng. C 70 (2017) 736–744.
[21] D.W. Lia, X. Lei, F.L. He, J. He, Y.L. Liu, Y.J. Ye, X. Deng, E. Duan, D.C. Yin, Silk fibroin/chitosan scaffold with tunable properties and low inflammatory response assists the differentiation of bone marrow mesenchymal stem cells, Int. J. Biol. Macromol. 105 (2017) 584–597.
[22] D.W. Li, F.L. He, J. He, X. Deng, Y.L. Liu, Y.Y. Liu, Y.J. Ye, D.C. Yin, From 2D to 3D: the morphology, proliferation and differentiation of MC3T3-E1 on silk fibroin/chitosan matrices, Carbohydr. Polym. 15 (178) (2017) 69–77.
[23] J. Wang, Q. Yang, N. Cheng, X. Tao, Z. Zhang, X. Sun, Q. Zhang, Collagen/silk fibroin composite scaffold incorporated with PLGA microsphere for cartilage repair, Mater. Sci. Eng. C 61 (1) (2016) 705–711.
[24] E. Szymańska, K. Winnicka, Stability of chitosan—a challenge for pharmaceutical and biomedical applications, Mar. Drugs 13 (4) (2015) 1819–1846.
[25] S.V. Madihally, H.W. Matthew, Porous chitosan scaffolds for tissue engineering, Biomaterials 20 (12) (1999) 1133–1142.
[26] Z. She, C. Jin, Z. Huang, B. Zhang, Q. Feng, Y. Xu, Silk fibroin/chitosan scaffold: preparation, characterization, and culture with HepG2 cell, J. Mater. Sci. Mater. Med. 19 (12) (2008) 3545–3553.
[27] A. Sionkowska, A. Płanecka, Preparation and characterization of silk fibroin/chitosan composite sponges for tissue engineering, J. Mol. Liq. 178 (2013) 5–14.
[28] H. Kweon, H.C. Ha, I.C. Um, Y.H. Park, Physical properties of silk fibroin/chitosan blend films, J. Appl. Polym. Sci. 80 (2001) 928–934.
[29] N. Kasoju, D. Kubies, M.M. Kumorek, J. Kríz, E. Fabryova, L. Machova, J. Kovarova, F. Rypáček, Dip TIPS as a facile and versatile method for fabrication of polymer foams with controlled shape size and pore architecture for bioengineering applications, PLoS One 9 (2014) 1–16.
[30] A.Y. Alentiev, Y.P. Yampolskii, Meares equation and the role of cohesion energy density in diffusion in polymers, J. Membr. Sci. 206 (2002) 291–306.
[31] G.T. Dee, B.B. Sauer, The surface tension of polymer blends: theory and experiment, Macromolecules 26 (11) (1993) 2771–2778.
[32] D.R. Paul, J.W. Barlow, A binary interaction model for miscibility of copolymers in blends, Polymer 25 (1984) 487–494.
[33] R. Jin, L.S. Moreira Teixeira, P.J. Dijkstra, M. Karperien, C.A. van Blitterswijk, Z.Y. Zhong, J. Feijen, Injectable chitosan-based hydrogels for cartilage tissue engineering, Biomaterials 30 (13) (2009) 2544–2551.
[34] J. Berger, M. Reist, J.M. Mayer, O. Felt, N.A. Peppas, R. Gurny, Structure and interactions in covalently and ionically crosslinked chitosan hydrogels for biomedical applications, J. Pharmacokinet. Biopharm. 57 (1) (2004) 19–34.
[35] I.L. Kim, R.L. Mauck, J.A. Burdick, Hydrogel design for cartilage tissue engineering: a case study with hyaluronic acid, Biomaterials 32 (34) (2011) 8771–8782.
[36] G.S. Huang, L.G. Dai, B.L. Yen, S.H. Hsu, Spheroid formation of mesenchymal stem cells on chitosan and chitosan-hyaluronan membranes, Biomaterials 32 (29) (2011) 6929–6945.
[37] L.E. Freed, G. Vunjak-Novakovic, R.J. Biron, D.B. Eagles, D.C. Lesnoy, S.K. Barlow, R. Langer, Biodegradable polymer scaffolds for tissue engineering, Biotechnology 12 (7) (1994) 689–693.
[38] J. Jaipaew, P. Wangkulangkul, J. Meesane, P. Ruangrat, P. Puttawibul, Mimicked cartilage scaffolds of silk fibroin/hyaluronic acid with stem cells for osteoarthritis surgery: morphological, mechanical, and physical clues, Mater. Sci. Eng. C 64 (2016) 173–182.
[39] Z.X. Cai, X.M. Mo, K.H. Zhang, L.P. Fan, A.L. Yin, C.L. He, H.S. Wang, Fabrication of Chitosan/Silk Fibroin Composite Nanofibers for Wound-dressing Applications, 11(9), 2010 3529–3539.
[40] N. Minoura, S.I. Aiba, M. Higuchi, Y. Gotoh, M. Tsukada, Y. Imai, Attachment and growth of fibroblast cells on silk fibroin, Biochem. Biophys. Res. Commun. 208 (2) (1995) 511–516.
[41] C. Vepari, D.L. Kaplan, Silk as a biomaterial, Prog. Polym. Sci. 32 (8–9) (2007) 991–1007.
[42] N. Minoura, M. Higuchi, M. Tsukada, Y. Imai, Attachment and growth of fibroblast cells on silk fibroin, Biochem. Biophys. Res. Commun. 208 (1995) 511–516.
[43] H. Ueno, H. Yamada, I. Tanaka, N. Kaba, M. Matsuura, M. Okumura, T. Kadosawa, T. Fujinaga, Accelerating effects of chitosan for healing at early phase of experimental open wound in dogs, Biomaterials 20 (15) (1999) 1407–1414.
[44] D.M. Cohen, B.T. Estes, J.M. Gimble, W. Liedtke, C.S. Chen, Control of stem cell fate by physical interactions with the extracellular matrix, Cell Stem Cell 5 (2009) 17–26.
[45] N. Bhardwaj, O.T. Nguyen, A.C. Chen, D.L. Kaplan, R.L. Sah, S.C. Kundu, Potential of 3-D tissue constructs engineered from bovine chondrocytes/silk fibroin-chitosan for in vitro cartilage tissue engineering, Biomaterials 32 (25) (2011) 5773–5781.
[46] D.E. Ashhurst, B.A. Ashton, M.E. Owen, The collagens and glycosaminoglycans of the extracellular matrices secreted by bone marrow stromal cells cultured in vivo in diffusion chambers, J. Orthop. Res. 8 (1990) 741–749.
[47] Y. Okamoto, M. Watanabe, K. Miyatake, M. Morimoto, Y. Shigemasa, S. Minam, Effects of chitin/chitosan and their oligomers/monomers on migrations of fibroblasts and vascular endothelium, Biomaterials 23 (9) (2002) 1975–1979.
[48] N. Bhardwaj, K.C. Kundu, Chondrogenic differentiation of rat MSCs on porous scaffolds of silk fibroin/chitosan blends, Biomaterials 33 (10) (2012) 2848–2857.